

See discussions, stats, and author profiles for this publication at: <https://www.researchgate.net/publication/51227753>

Nanostructured Growth Patterns and Chaotic Oscillations in Potential during Electropolymerization of Aniline in the Presence of Surfactants

ARTICLE *in* THE JOURNAL OF PHYSICAL CHEMISTRY B · JUNE 2011

Impact Factor: 3.3 · DOI: 10.1021/jp1095757 · Source: PubMed

CITATIONS

7

READS

28

4 AUTHORS, INCLUDING:



Rinki Choudhary

Deen Dayal Upadhyaya Gorakhpur University

8 PUBLICATIONS 112 CITATIONS

SEE PROFILE

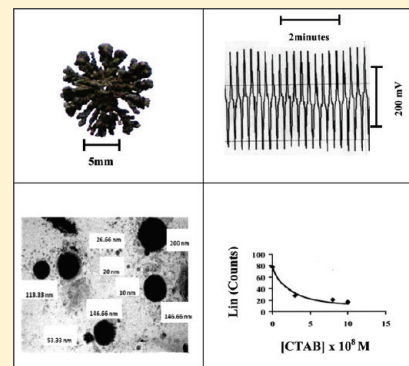
Nanostructured Growth Patterns and Chaotic Oscillations in Potential during Electropolymerization of Aniline in the Presence of Surfactants

Ishwar Das,^{*†} Rinki Choudhary, Sanjeev Kumar Gupta, and Pranav Agrawal[‡]

[†]Chemistry Department, DDU Gorakhpur University, Gorakhpur-273009, India

[‡]Department of Chemical Engineering, Indian Institute of Technology, Kanpur-208016, India

ABSTRACT: Polyaniline nanoparticles were synthesized by simple electrochemical polymerization of aniline in systems (a) aniline–sodium dodecyl sulfate (NaDS)–dodecylbenzene sulfonic acid (DBSA)–H₂O and (b) aniline–NaDS–DBSA–cetyltrimethyl ammonium bromide (CTAB)–H₂O. Different morphologies including compact and fractal/dendrimer were observed at different experimental conditions. Fractal dimension was calculated by the box counting method. Growth kinetics during electropolymerization of aniline in both of the systems was studied by measuring the weight of polymer aggregates as a function of time. Growth rate was found to be reduced in system (b) due to coordination of CTAB with the growing polyaniline chain. The weight of polymer aggregates was found to depend on field intensity and attains a maximum value at a critical field intensity 4.0 V/cm. Beyond this critical field intensity, the growth rate was decreased due to loss of conjugation and degradation of the polymer backbone. Electropolymerized aggregates were characterized by transmission electron microscopy (TEM), powder X-ray diffraction (XRD), Fourier transform infrared spectroscopy (FT-IR), and electrical conductivity measurements. Nanosized polyaniline was formed, with particle diameters in the range of 10–200 nm, as evident by TEM studies and supported by XRD studies. FT-IR spectroscopy established the formation of hyperbranched polyaniline chains. During electropolymerization, oscillations in potential were monitored as a function of time at different experimental conditions. A suitable mechanism for fractal growth of polyaniline was also proposed.



INTRODUCTION

Electrochemical reaction with nonlinear kinetics gives rise to various dynamic self-organization phenomena such as oscillation and spatiotemporal pattern formation.^{1,2} Far from equilibrium phenomena such as electric potential oscillation, chaos and fractal growth are of considerable current interest during recent years.^{3–8} Metal electrodeposition^{1,5–7,9,10} and electropolymerization^{4,11,12} at an air liquid interface have attracted a great deal of attention from the point of view of morphologies and electric potential oscillation. The formation of dendrites, dendrimers, and hyperbranched polymers occurs in natural phenomena. Conducting polymers with large π conjugation structure have received considerable attention due to their potential applications in science and technology^{16–22} including biological sensing.²³ In particular, polyaniline is a very attractive material due to its chemical stability, easy polymerization, and promising applications in electronic devices^{24,25} such as rechargeable batteries, conducting coatings, electromagnetic shielding, and gas separation membranes. Different nano- and microscale structures of polyaniline were produced from the chemical oxidation of aniline. Details are given in a recent review by Tran et al.²⁶ A number of investigations have been devoted to the study of chemical and electrochemical polymerization of aniline with and without surfactants^{27–36} in inorganic acidic medium. However, electrochemical methods of polymerization of aniline with surfactants in the absence of any inorganic acid are lacking.

In this communication, we have investigated the transitions in structures obtained during electropolymerization of aniline in

aqueous solutions of mixed surfactants sodium dodecyl sulfate (NaDS), dodecylbenzene sulfonic acid (DBSA) and NaDS containing DBSA and cetyltrimethylammonium bromide (CTAB). Growth kinetics under different experimental conditions was also studied. Electropolymerized aggregates were characterized by transmission electron microscopy (TEM), powder X-ray diffraction (XRD), Fourier transform infrared spectroscopy (FT-IR), and electrical conductivity studies. During electropolymerization, electric potential was monitored as a function of time at different experimental conditions. A suitable mechanism for fractal growth of polyaniline was also proposed.

EXPERIMENTAL SECTION

Aniline (s.d. fine-chem. Ltd., AR), NaDS (s.d. fine-chem. Ltd., LR), DBSA (Fluka, AR), and CTAB (s.d. fine-chem. Ltd.) were used as received.

Electrochemical Synthesis, Morphology and Growth Kinetics. The aniline was electrochemically polymerized at 30.0 ± 0.1 °C in an incubator using an experimental set up consisting of a Petri dish containing a solution of aniline, water, and the surfactant, NaDS and DBSA, in the absence and presence of a cationic surfactant CTAB. Five milliliters of the solution was taken in the Petri dish. A cleaned platinum circular cathode of

Received: October 6, 2010

Revised: May 2, 2011

Published: June 17, 2011

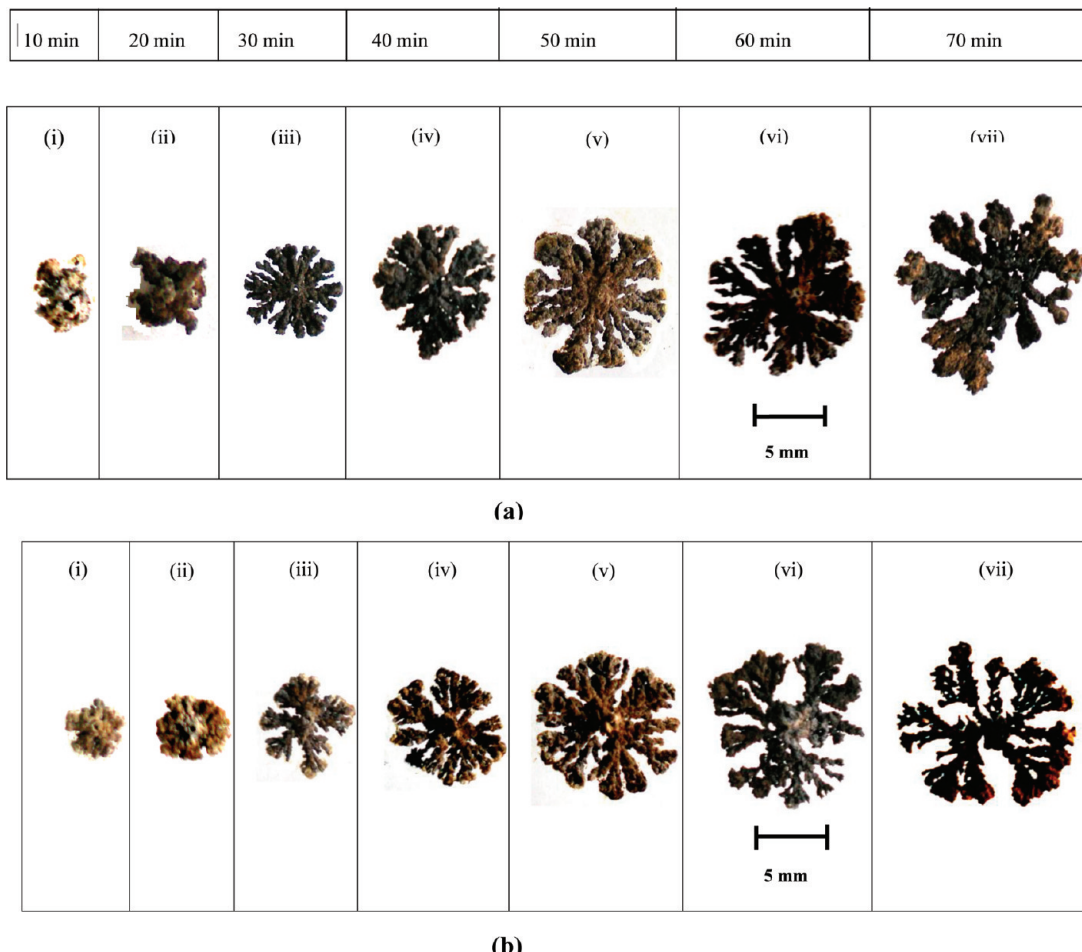


Figure 1. Microphotographs obtained during electropolymerization of aniline as a function of time in systems (a) aniline–NaDS–DBSA–H₂O and (b) aniline–NaDS–DBSA–CTAB–H₂O at 10, 20, 30, 40, 50, 60, and 70 min, respectively (i–vii). Conditions: [Aniline] = 0.5M, [NaDS] = 0.1M, [DBSA] = 6×10^{-4} M, [CTAB] = 3×10^{-8} M, field intensity 3.6 V/cm.

radius 2.5 cm was immersed in the solution, while the platinum vertical anode (diameter 0.34 mm) was put at an air/liquid interface at the center of the circular cathode of radius 2.5 cm in all experiments. Thus the distance between electrodes was 2.5 cm in each case. These electrodes were attached to a DC digital potentiostat (Scientific, India) to supply constant potential. Polymerization started at the tip of the anode immediately on applying the potential across the electrodes. Electropolymerization was carried out at moderate potential to prevent the oxidative decomposition of the solvent, electrolyte, and the monomer. At the end of experiment, the material was detached gently from the tip of the anode. Polymer was synthesized at different times of polymerization, field intensities, and surfactant concentrations. Field intensity was varied in the range 1.2–4.6 V/cm, while [DBSA] was varied in the range 6×10^{-4} to 20×10^{-4} M. Aggregates were photographed with a digital camera. The growth kinetics was studied by weighing the washed and dried aggregates as a function of time of polymerization and other experimental conditions, viz. field intensity, [DBSA], and [CTAB].

Electrical Conductivity Measurements. Electrical conductivity of electropolymerized aggregates obtained from (a) aniline–NaDS–DBSA–H₂O and (b) aniline–NaDS–DBSA–CTAB–H₂O systems, were measured at room temperature at different times

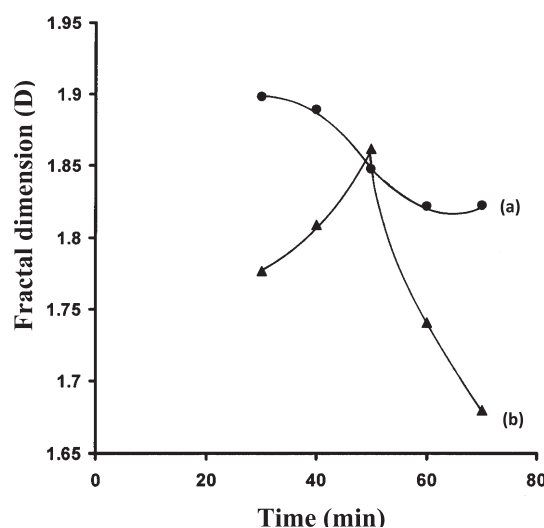


Figure 2. Dependence of fractal dimension (D) on time for polymer aggregates obtained in systems (a) and (b) after 30 min of polymerization. Conditions: [Aniline] = 0.5M, [NaDS] = 0.1M, [DBSA] = 6×10^{-4} M, [CTAB] = 3×10^{-8} M, field intensity 3.6 V/cm.

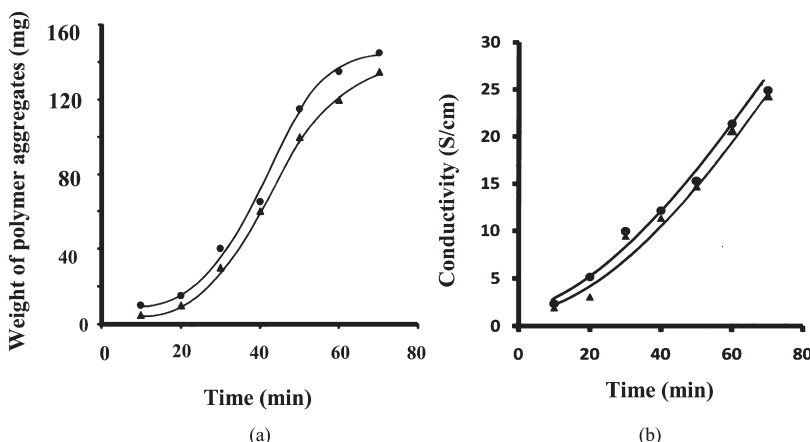
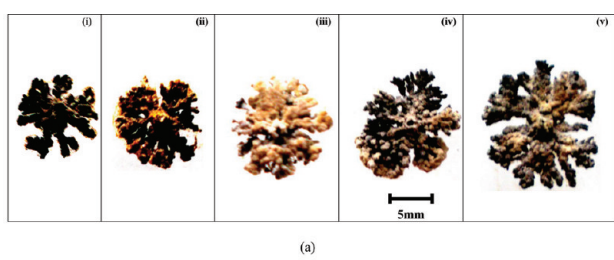
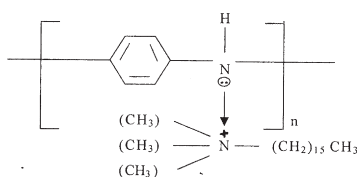
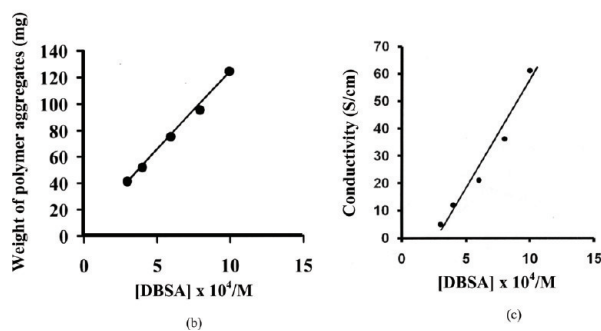


Figure 3. (a) Growth kinetics, and (b) electrical conductivity data for polymer aggregates obtained during electropolymerization in systems (●) aniline–NaDS–DBSA–H₂O and (▲) aniline–NaDS–DBSA–CTAB–H₂O. Conditions: [Aniline] = 0.5M, [NaDS] = 0.1M, [DBSA] = 6×10^{-4} M, [CTAB] = 3×10^{-8} M, field intensity 3.6 V/cm.

Scheme 1



(a)

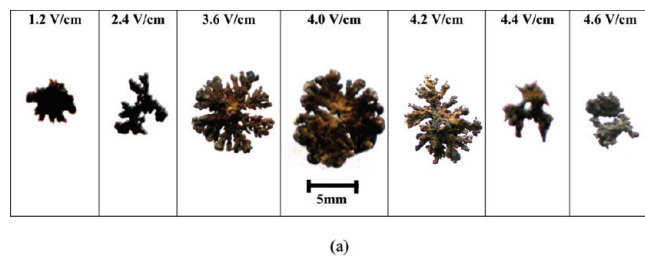


(b)

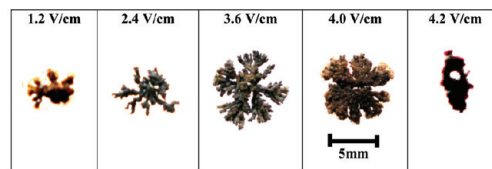
(c)

Figure 4. Microphotographs (a), weight of polymer aggregates (b), and electrical conductivity (c) of polymer aggregates obtained during electropolymerization of the aniline–NaDS–DBSA–H₂O system at different DBSA concentrations. Conditions: [Aniline] = 0.5M, [NaDS] = 0.1M, [DBSA] = 6×10^{-4} M to 20×10^{-4} M. Field intensity = 3.6 V/cm. Time of polymerization = 30 min.

using an experimental setup consisting of a glass capillary (inner diameter = 1.4 mm) filled with the solid sample with a fixed length of 1 cm. Two bright platinum electrodes of diameter 0.34 mm were



(a)



(b)

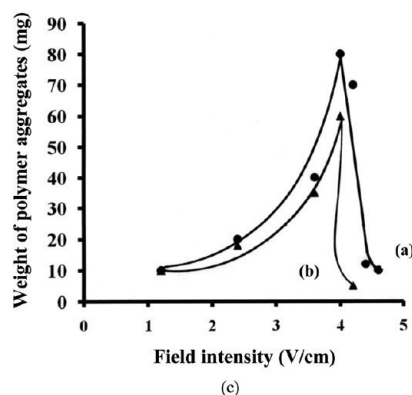


Figure 5. Microphotographs (a, b), and dependence of weight of electropolymerized aggregates (c) at different field intensities up to 4.6 V/cm in systems (a) aniline–NaDS–DBSA–H₂O and (b) aniline–NaDS–DBSA–CTAB–H₂O. Conditions: [Aniline] = 0.5M, [NaDS] = 0.1M, [DBSA] = 6×10^{-4} M, [CTAB] = 10×10^{-8} M. Time of polymerization = 30 min.

inserted into the capillary such that these touched the sample and connected to a conductivity meter.

Computation of Fractal Dimension D. Fractal aggregates were photographed and scanned with the help of a scanner attached to a computer. Experiments were repeated several

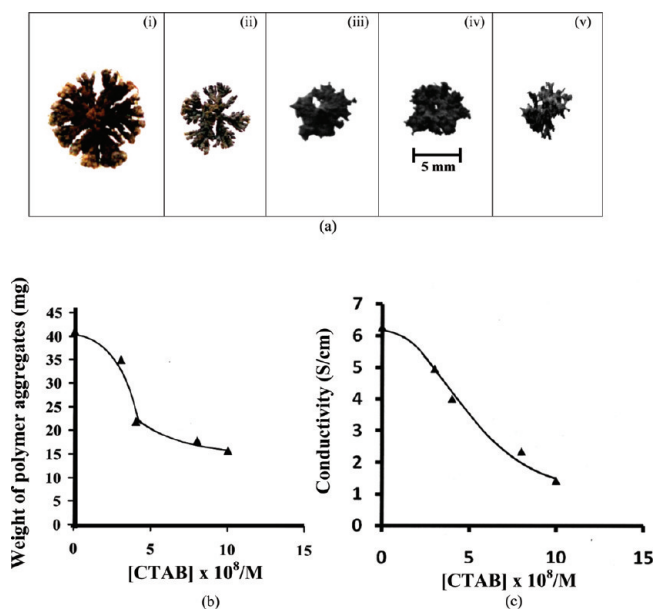


Figure 6. (a) Microphotographs, (b) weight, and (c) electrical conductivity of polymer aggregates obtained during electropolymerization of aniline–NaDS–DBSA–CTAB– H_2O systems at different [CTAB]. Conditions: [Aniline] = 0.5M, [NaDS] = 0.1M, [DBSA] = 6×10^{-4} M, [CTAB] = 3×10^{-8} to 10×10^{-8} M, field intensity = 3.6 V/cm. Time of polymerization = 30 min.

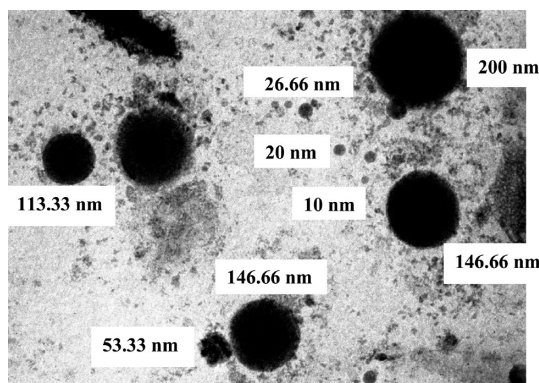


Figure 7. TEM image of electropolymerized aggregates obtained from the aniline–NaDS–DBSA– H_2O system. Conditions: [Aniline] = 0.5M, [NaDS] = 0.1M, field intensity = 3.6 V/cm. Time of polymerization = 30 min.

times. The fractal dimension D of reproduced aggregates was determined by box counting methods.³⁷ The total number of boxes $N(r)$ is related to the radius r by the relation $N(r) \sim r^D$. Fractal dimension D was obtained by plotting $\log N(r)$ against $\log r$ using the method of least-squares analysis.

TEM Studies. TEM images of polymer aggregates obtained during electropolymerization of aniline from the aniline–NaDS–DBSA– H_2O system employing a circular cathode and a vertical anode were taken using a Philips transmission electron microscope (model CM 200).

XRD Studies. XRD patterns of electrochemically synthesized polymer aggregates obtained from aniline–NaDS–DBSA– H_2O and aniline–NaDS–DBSA–CTAB– H_2O systems at different

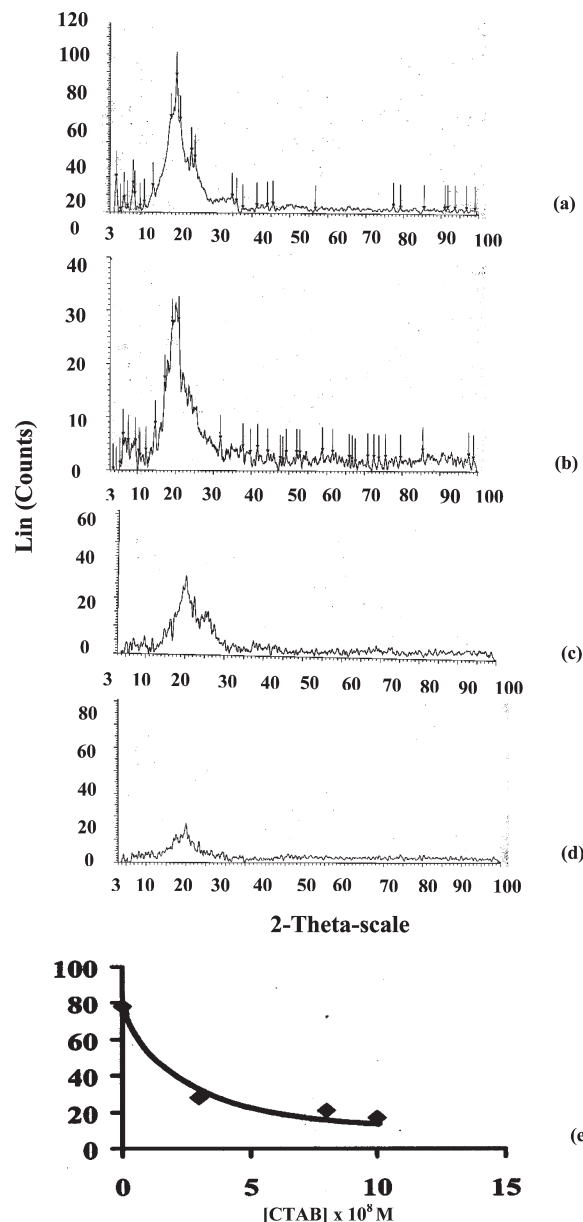


Figure 8. XRD patterns of polymer aggregates obtained from aniline–NaDS–DBSA– H_2O (a) and aniline–NaDS–DBSA–CTAB– H_2O systems at different [CTAB] (b–d). Conditions: [Aniline] = 0.5M, [NaDS] = 0.1M, [DBSA] = 6×10^{-4} M, [CTAB] = 3×10^{-8} to 10×10^{-8} M, field intensity = 3.6 V/cm. Time of polymerization = 30 min. Dependence of relative intensity of peak on [CTAB] is shown in panel e.

[CTAB] were taken in the 2θ range 0 – 100° using a Bruker X-ray diffractometer, model D-8.

FT-IR Spectroscopy. FT-IR spectrum of the polymer aggregate obtained from the aniline–NaDS–DBSA– H_2O system synthesized at 3.6 V/cm was taken using a Nicolet Instruments Corporation (USA) FT-IR spectrometer, model MAGNA 550.

Oscillations in Anode Potential with Time during Electropolymerization. The potential between the anode and the reference standard calomel electrode during electropolymerization of aniline in (a) aniline–NaDS–DBSA– H_2O and (b) aniline–NaDS–DBSA–CTAB– H_2O systems was monitored as a function of time at different experimental conditions.

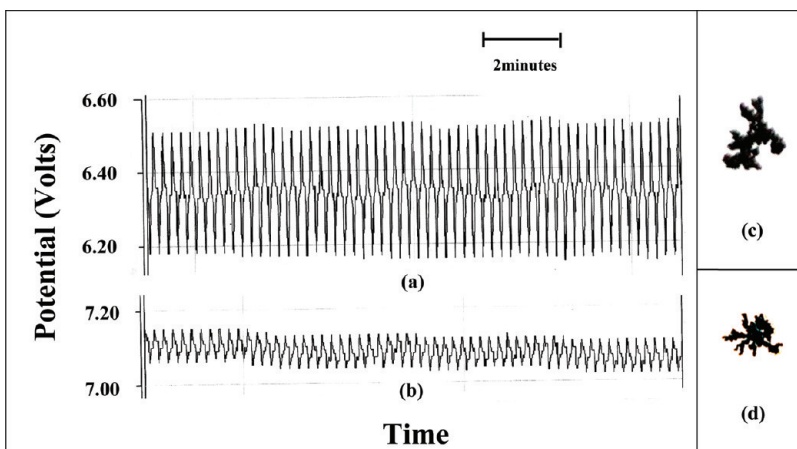


Figure 9. Anode potential changes with time (a,b) and corresponding morphologies of the polymer aggregates (c,d) obtained during electropolymerization of aniline in systems (a) and (b), respectively. Conditions: [Aniline] = 0.5 M; [NaDS] = 0.1 M; [DBSA] = 6×10^{-4} M; [CTAB] = (a) 0, (b) 6×10^{-8} M; field intensity = 3.6 V/cm.

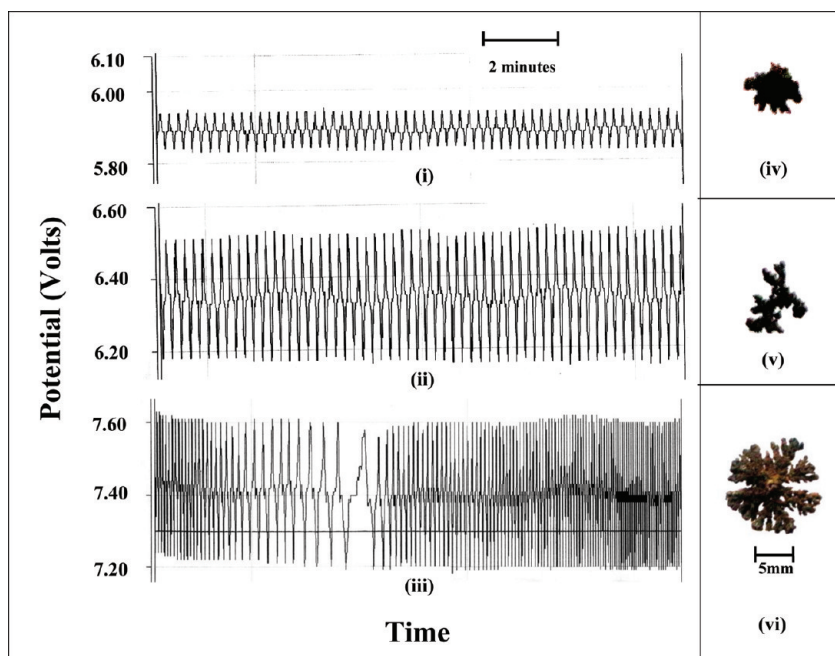


Figure 10. Anode potential changes with time (i–iii) and corresponding morphologies (iv–vi) obtained during electropolymerization of aniline in aniline–NaDS–DBSA–H₂O system at different field intensities. Conditions: [Aniline] = 0.5 M; [NaDS] = 0.1 M; [DBSA] = 6×10^{-4} M; field intensity = 1.2 V/cm (i,iv), 2.4 V/cm (ii,v), and 3.6 V/cm (iii,vi).

Potential measurements were made with the help of a paperless x-t recorder, model VM 7003A0000 (Ohkura Electric Co. Ltd., Japan). The experiment was conducted in a flat-bottom Corning Petri dish consisting of two platinum electrodes, separated by 2.5 cm. The circular cathode was extended below the surface of the solution, whereas the lower end of the vertical anode was put at the surface.

RESULTS AND DISCUSSION

Complex structures were produced during electropolymerization of aniline in the presence of (a) anionic surfactant NaDS containing DBSA and (b) NaDS and DBSA containing a cationic surfactant CTAB, at different times. Growth morphologies are

shown in Figure 1. Initially, the growth was compact and after 20 min, a transition from compact to fractal was observed in each case due to the process of diffusion-limited aggregation. Diffusion limited aggregation is a process wherein successive particles move in space and undergo a random walk until they interact with a growing fractal, resulting in a tree like structure. The time dependence of the fractal dimension of polymer aggregates obtained during electropolymerization of systems (a) and (b) is shown in Figure 2. The data are plotted as D versus time. In the case of system (a), the fractal dimension was found to decrease with time (Figure 2a), while in the case of system (b), the fractal dimension first increased, attained a threshold value at 50 min, and then decreased (Figure 2b). The growth kinetics of polymerization was investigated by measuring the weight of aggregates

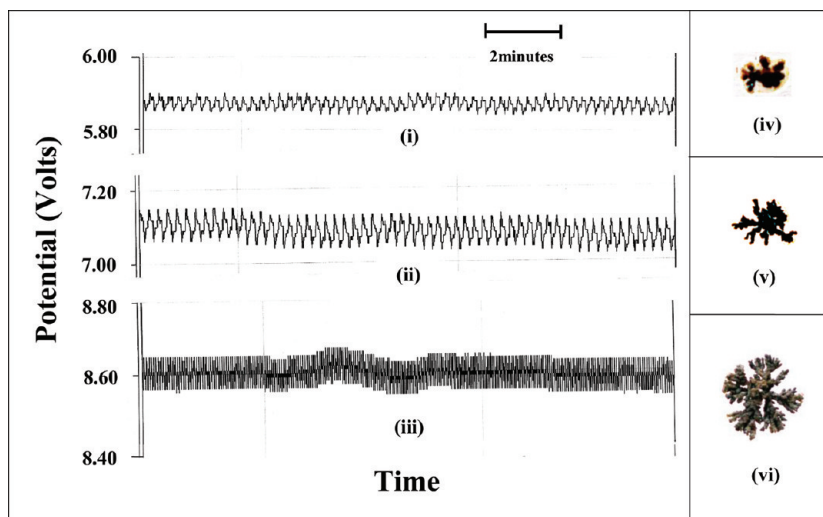


Figure 11. Anode potential changes with time (i–iii) and corresponding morphologies (iv–vi) obtained during electropolymerization of aniline in the aniline–NaDS–DBSA–CTAB–H₂O system at different field intensities. Conditions: [Aniline] = 0.5 M; [NaDS] = 0.1 M; [DBSA] = 6 × 10⁻⁴ M; [CTAB] = 6 × 10⁻⁸ M; field intensity = 1.2 V/cm (i,iv), 2.4 V/cm (ii,v), and 3.6 V/cm (iii,vi).

at different times, keeping other parameters fixed. Results are shown in Figure 3a. As the time of polymerization was increased, after an induction period, a sharp increase in the growth rate was observed due to continuous electrooxidation of aniline monomer present in the medium, leading to greater molecular mass and larger π -conjugation of the growing polymer chain. It is also observed that the growth reduction on addition of CTAB in the medium may be due to coordination of CTAB with the growing polyaniline chain as shown in Scheme 1.

In order to confirm the above observations, electrical conductivity of the polymer aggregates was measured, and results are shown in Figure 3b. In the absence of CTAB, electrical conductivity was higher, possibly due to large π -conjugation of the growing polymer chain, while in the presence of CTAB electrical conductivity was reduced because of the coordination of CTAB with the growing polyaniline chain.

Morphologies and growth kinetics were also studied at different [DBSA], field intensity, and [CTAB]. Results are shown in Figures 4–6. Dependence of fractal growth morphologies on [DBSA] is shown in Figure 4a. Increment in [DBSA] in the medium results in an increase in the anodic charge of the film and leads to better protonation of polyaniline³⁸ favorable for the formation of polyaniline with large π -conjugation, as evident by the increase in the polymer yield (Figure 4b) and electrical conductivity values (Figure 4c). Dependence of growth morphology on field intensity for systems (a) aniline–NaDS–DBSA–H₂O and (b) aniline–NaDS–DBSA–CTAB–H₂O is shown in Figure 5a,b. The corresponding weights of the polymer aggregates were also measured, and the results are shown in Figure 5c. The applied potential introduces the effect on the structure and properties of electrogenerated polyaniline and the rate of polymer production. It attains a maximum value at critical field intensity 4.0 V/cm, both in the absence and presence of CTAB. Beyond this critical field intensity, the growth rate was decreased, possibly due to loss of π -conjugation and degradation of polymer backbone. It is also evident that, in the presence of CTAB, the growth rate was reduced due to coordination of CTAB with the growing polymer chain. Dependence of growth morphologies and growth kinetics on [CTAB] is shown in Figure 6. On increasing [CTAB] in the medium, the growth rate was decreased,

and then it attains a constant value (Figure 6b). The electrical conductivity of polymer follows the same trend as shown in Figure 6c. It may be due to the decrease in the weight of polymer and π -conjugation of the growing polymer chain in the presence of CTAB. On further addition of CTAB, it attains a constant value due to nonavailability of a lone pair of electrons on the nitrogen atom of the polyaniline.

Electropolymerized aggregate obtained from system (a) was characterized by TEM and XRD studies. TEM studies revealed the formation of nanosized particles with particle diameters in the range 10–200 nm (Figure 7). Particle diameter (t_{hkl}) was also calculated by XRD studies using the Debye–Scherrer formula:³⁹

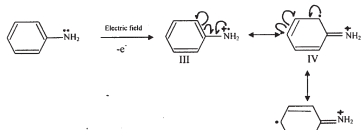
$$t_{hkl} = \frac{0.9\lambda}{3\beta \cos \theta_\beta} \frac{360}{2\pi} \text{\AA}$$

where β = half-maximum width, λ = wavelength, and θ_β = Bragg's angle corresponding to the β value.

The particle diameter was found to be 16 nm, in agreement with the TEM results. Influence of [CTAB] on XRD patterns has also been studied. [CTAB] was varied in the range 3 × 10⁻⁸ to 10 × 10⁻⁸ M. It is observed that relative intensity of the peak at 2θ = 20.190° was gradually decreased with increase in [CTAB] (Figure 8e) following the same trend as observed in their conductivity values (Figure 6c).

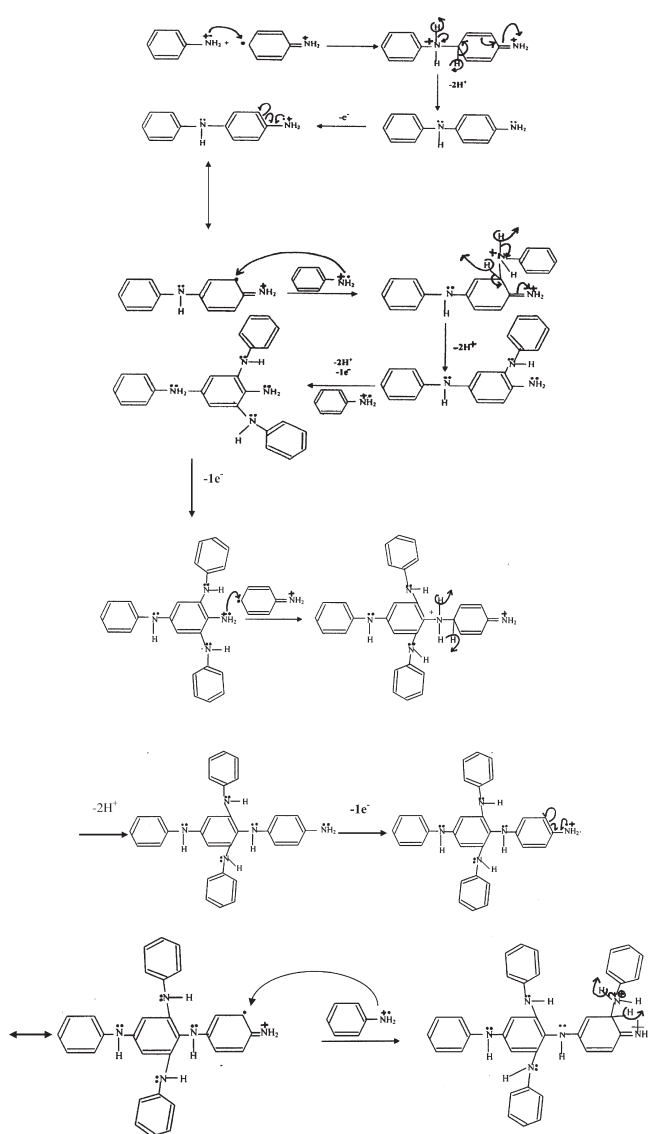
Change in potential with time in (a) aniline–NaDS–DBSA–H₂O and (b) aniline–NaDS–DBSA–CTAB–H₂O systems along with their corresponding morphologies obtained during electropolymerization were recorded. Results are shown in Figures 9–11. In the absence of CTAB, it was observed that the absolute value of potential was less, while the amplitude of oscillation was more (Figure 9). It is also observed that the amplitude of oscillation and weight of polymer aggregate were interrelated. The higher the amplitude of chaotic oscillation, the higher the weight of polymer aggregate (Figure 9). Figure 10 shows the change in potential with time and corresponding morphologies obtained at different field intensities in the range 1.2–3.6 V/cm during electropolymerization of aniline in the absence of CTAB. At low field intensity (1.2 V/cm) (Figure 10i), the amplitude and frequency were small, while at higher field

(i) Formation of radical cation from electrooxidation of aniline at the surface of electrode:



(ii) Combination of radical cations generated in step (i) with another radical cation to form dimer.

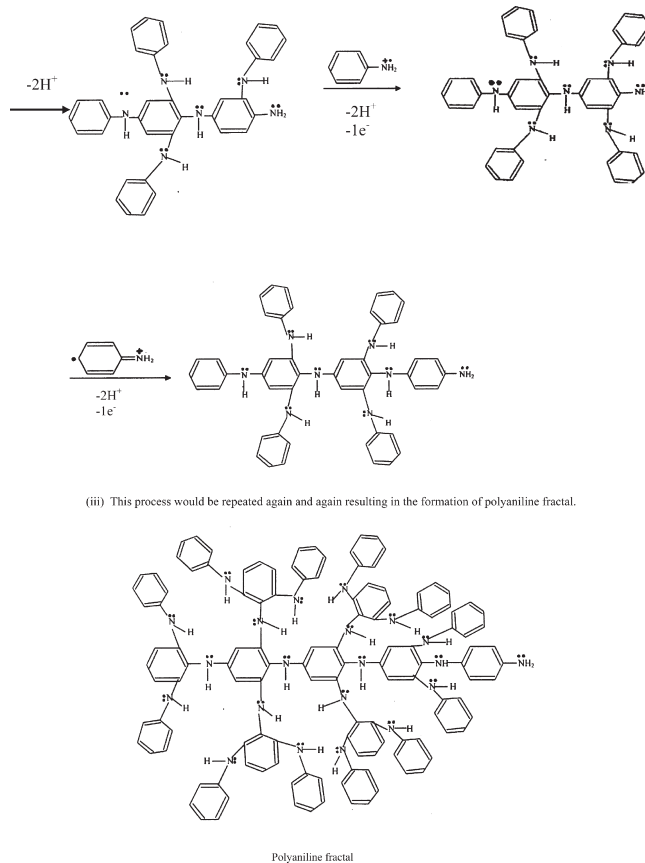
The process would be repeated to form fractal polyaniline.



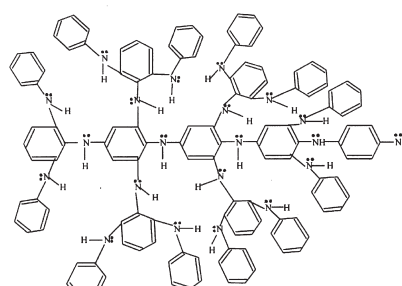
intensity (3.6 V/cm) (Figure 10iii), the amplitude and frequency of oscillation were increased. Weight of polymer aggregate was also increased with increase in field intensity (Figure 10iv–vi). A similar trend was also observed when the above experiment was performed in the presence of CTAB (Figure 11).

The mechanism of development of electric potential oscillations and fractal growth of polyaniline may be understood as follows: Electropolymerization proceeds through successive electrochemical and chemical steps. It includes the oxidation of the monomer to form a radical cation. When the current is passed through the system, aniline radical cation is formed from aniline with the release of one electron so that the free radical is attracted toward the anode. This promotes the passage of electric current through the system. These free radicals undergo chain polymerization followed by the deposition

of the polymer on anode and thus decrease in potential. When aniline cation is in excess, electrical potential increases. On the other hand, on polymerization, the effective concentration of aniline radical cation decreases, leading to decrease in potential. When enough aniline radical cation gets accumulated, the cycle is repeated again and again, but in a nonperiodic manner. Thus chaotic oscillations were observed. The detailed steps of the mechanism may be understood as follows:



(iii) This process would be repeated again and again resulting in the formation of polyaniline fractal.



Polyaniline fractal

The formation of hyperbranched polyaniline chains has been established by FT-IR spectroscopy exhibiting peaks in the substitution region of wave numbers $900\text{--}650 \text{ cm}^{-1}$ ($668.59, 692.10, 750.00$, and 814.74 cm^{-1}) attributed to the out-of-plane bending motion of C–H of substituted benzene nuclei.⁴⁰ The fractal geometry is generated by the microscopic growth pattern moving through the solution. TEM illustrates that the primary nanoparticles are spherical. The fractal geometry on the micro-meter/millimeter length scale is probably caused by the aggregation of such nanoparticles as polyaniline grows out through the solution in a fractal manner.

CONCLUSIONS

Nanostructured polyaniline was synthesized by simple electrochemical polymerization of aniline in the presence of mixed surfactants. Compact and fractal/dendrimer morphologies were obtained at different experimental conditions. Growth rate was inhibited in the presence of a cationic surfactant CTAB due to its coordination with growing polyaniline chain. Electropolymerized aggregates were characterized by TEM, XRD, FT-IR, and electrical conductivity measurements. TEM and XRD studies revealed the formation of nanosized polyaniline particles in the range $10\text{--}200 \text{ nm}$. The formation of a hyperbranched polyaniline

chain was established by FT-IR spectroscopy. Oscillations in potential during electropolymerization were chaotic in nature in all the cases. A mechanism for fractal growth of polyaniline was proposed.

AUTHOR INFORMATION

Corresponding Author

*Tel: +91-551-2338731. Fax: +91-551-2342880. E-mail: ishwar_das@rediffmail.com.

ACKNOWLEDGMENT

We thank the learned reviewers for constructive and helpful suggestions. I.D. is thankful to the University Grants Commission, New Delhi for supporting Project No. F 37-135/2009/SR, and the Head of the Chemistry Department, D. D. U. Gorakhpur University, Gorakhpur, India, for providing necessary laboratory facilities. We also thank IIT Bombay for providing TEM results and NIPER, Mohali, for XRD studies.

REFERENCES

- (1) Nakanishi, S.; Nagai, T.; Fukami, K.; Sonoda, K.; Oka, N.; Ihara, D.; Nakato, Y. *Langmuir* **2008**, *24*, 2564.
- (2) Christoph, J.; Eiswirth, M. *Chaos* **2002**, *12* (1), 215.
- (3) Rastogi, R. P. *Introducion to Non-equilibrium Physical Chemistry: Towards Complexity and Non-linear Science*; Elsevier: Amsterdam, 2008.
- (4) Kaufman, J. H.; Melroy, O. R.; Abraham, F. F.; Nazzal, A. I. *Solid State Commun.* **1986**, *60* (9), 757.
- (5) Fukami, K.; Nakanishi, S.; Yamasaki, H.; Tada, T.; Sonoda, K.; Kamikawa, N.; Tsuji, N.; Sakaguchi, H.; Nakato, Y. *J. Phys. Chem. C* **2007**, *111*, 1150.
- (6) Nakanishi, S.; Fukami, K.; Tada, T.; Nakato, Y. *J. Am. Chem. Soc.* **2004**, *126*, 9556.
- (7) Rastogi, R. P.; Das, I.; Pushkarna, A.; Chand, S. *J. Phys. Chem. B* **1993**, *97*, 4871.
- (8) Das, I.; Verma, S.; Ansari, S. A.; Lall, R. S.; Agrawal, N. R. *Fractals* **2010**, *18*, 215.
- (9) Das, I.; Ansari, S. A. *J. Ind. Chem. Soc.* **2010**, *87*, 1.
- (10) Chazaiviel, J. N.; Fleury, V.; Rosso, M. *Trends Electrochem.* **1992**, *1*, 231.
- (11) Das, I.; Agrawal, N. R.; Ansari, S. A.; Gupta, S. K. *Indian J. Chem.* **2008**, *47A*, 1798.
- (12) Das, I.; Agrawal, N. R.; Gupta, S. K.; Gupta, S. K.; Rastogi, R. P. *J. Phys. Chem. A* **2009**, *113*, 5296.
- (13) Li, X.-G.; Hou, Z.-Z.; Huang, M.-R.; Moloney, M. G. *J. Phys. Chem. C* **2009**, *113*, 21586.
- (14) Li, X.-G.; Wei, F.; Huang, M.-R.; Xie, Y.-B. *J. Phys. Chem. B* **2007**, *111*, 5829.
- (15) Li, X.-G.; Li, J.; Huang, M.-R. *Chem.—Eur. J.* **2009**, *15*, 6446.
- (16) Zhang, H.; Wang, J.; Wang, Z.; Zhang, F.; Wang, S. *Synth. Met.* **2009**, *159*, 277.
- (17) Virji, S.; Huang, J. X.; Kaner, R. B.; Weiller, B. H. *Nano Lett.* **2004**, *4* (3), 491.
- (18) Wang, Y. G.; Li, H. Q.; Xia, Y. Y. *Adv. Mater.* **2006**, *18* (19), 2619.
- (19) Abbas, S. M.; Dixit, A. K.; Chatterjee, R.; Goel, T. C. *J. Nanosci. Nanotechnol.* **2007**, *7* (6), 2129.
- (20) Adhikari, A.; Claesson, P.; Pani, J.; Leygraf, C.; Deidinaitei, A.; Blomberg, E. *Electrochim. Acta* **2008**, *53* (12), 4239.
- (21) Chen, C. C.; Hwang, S. R.; Li, W. H.; Lee, K. C.; Chi, G. C.; Hsiao, H. T.; Wu, C. G. *Polym. J.* **2002**, *34* (4), 271.
- (22) de Barros, R. A.; Martins, C. R.; de Azevedo, W. M. *Synth. Met.* **2005**, *155* (1), 35.
- (23) Li, J.; Kendig, C. E.; Nesterov, E. E. *J. Am. Chem. Soc.* **2007**, *129*, 15911.
- (24) MacDiarmid, A. G.; Epstein, A. J. *Faraday Discuss. Chem. Soc.* **1989**, *88*, 317.
- (25) Kaneko, M.; Nakamura, H. *J. Chem. Soc. Chem. Commun.* **1985**, 1441.
- (26) Tran, H. D.; D'Arcy, J. M.; Wang, Y.; Beltramo, P. J.; Strong, V. A.; Kaner, R. B. *J. Mater. Chem.* **2011**, *21*, 3534.
- (27) Han, Y.-G.; Kusunose, T.; Sekino, T. *Synth. Met.* **2009**, *159*, 123.
- (28) Rahy, A.; Yang, D. *J. Mater. Lett.* **2008**, *62*, 4311.
- (29) Dallas, P.; Stamopoulos, D.; Boukos, N.; Tzitzios, V.; Niarchos, D.; Petridis, D. *Polymer* **2007**, *48*, 3162.
- (30) Kahol, P. K.; Satheesh Kumar, K. K.; Geetha, S.; Trivedi, D. C. *Synth. Met.* **2003**, *139*, 191.
- (31) Sapurina, I.; Stejskal, J.; Spirkova, M.; Kotek, J.; Prokes, J. *Synth. Met.* **2005**, *151*, 93.
- (32) Prasannan, A.; Truong, T.; Le, B.; Hong, P. D.; Somanathan, N.; Shown, I.; Imae, T. *Langmuir* **2011**, *27* (2), 766.
- (33) Maranhao, S. L. D. A.; Torresi, R. M. *Electrochim. Acta* **1999**, *44*, 1879.
- (34) Cai, L. T.; Yao, S. B.; Zhou, S. M. *Synth. Met.* **1997**, *88*, 209.
- (35) Kanungo, M.; Kumar, A.; Contractor, A. Q. *J. Electroanal. Chem.* **2002**, *528*, 46.
- (36) Michaelson, J. C.; McEvoy, A. J.; Kuramoto, N. *React. Polym.* **1992**, *17*, 197.
- (37) Rastogi, R. P.; Das, I.; Pushkarna, A.; Sharma, A.; Jaiswal, K.; Chand, S. *J. Chem. Educ.* **1992**, *69* (2), A47.
- (38) Taka, T.; Laakso, J.; Levon, K. *Solid State Commun.* **1994**, *92* (5), 393.
- (39) Klug, P. H.; Alexender, L. E. *X-ray Diffraction Procedures*; John Wiley & Sons, Inc: New York, 1954; p 512.
- (40) Li, X.-G.; Huang, M.-R.; Duan, W.; Yang, Y.-L. *Chem. Rev.* **2002**, *102*, 2925.